Rate Constants of the Reaction of NO_3 with CH_3I Measured with Use of Cavity Ring-Down Spectroscopy

Yukio Nakano* and Takashi Ishiwata

Faculty of Information Sciences, Hiroshima City University, Hiroshima 731-3194, Japan

Masahiro Kawasaki

Department of Molecular Engineering and Graduate School of Global Environmental Studies, Kyoto University, Kyoto 615-8510, Japan

Received: April 8, 2005; In Final Form: May 30, 2005

We have applied cavity ring-down spectroscopy to a kinetic study of the reaction of NO_3 with CH_3I in 20−200 Torr of N_2 diluent at 298 K. The rate constant of the reaction of $NO_3 + CH_3I$ was determined to be $(4.1 \pm 0.2) \times 10^{-13}$ cm^3 molecule^{-1} s^{-1} in 100 Torr of N_2 diluent at 298 K and is pressure-independent. This reaction may significantly contribute to the formation of reactive iodine compounds in the atmosphere.

1. Introduction

Reactive iodine compounds, such as iodine monoxide (IO) radical are important to the iodine cycle in the atmosphere of the Earth.[1,2] For example, IO affects the oxidizing capacity of the atmosphere because it is involved in the ozone depleting cycle as an efficient oxidizer, and is formed from the sequential reactions of alkyl iodides in the marine boundary layer.[3−6] Alkyl iodides are produced by various types of macroalgae and phytoplankton in the ocean and emitted into the atmosphere. Among them, methyl iodide (CH_3I) is most abundant in the atmosphere. After CH_3I is released into the atmosphere, it is rapidly photolyzed within a few days to form reactive iodine compounds.[7,8] The other atmospheric consumption pathway is the reaction with OH radicals. Since the rate constant is around 10^{-13} cm^3 molecule^{-1} s^{-1} at 298 K, this reaction accounts for 5% of the overall loss.[9]

At nighttime, IO is considered to be absent in the marine boundary layer, because it is mainly formed from the sunlight photolysis of alkyl iodides. However, Saiz-Lopez and Plane have reported the observations of I_2, OIO, IO, and nitrate radical (NO_3) with use of differential optical absorption spectroscopy at the Mace Head Atmospheric Research Station on the west coast of Ireland during August 2002.[10] They also reported a significant concentration of the iodine oxides during the nighttime. For example, the mixing ratios of IO rose to a maximum of 7 ppt. They suggested that the reaction between NO_3 and I_2 has an important role on the generation of IO and OIO because the measured mixing ratio for NO_3 was 7 ppt. Even if the mixing ratios of I_2 and NO_3 are assumed to be 50 and 7 ppt, respectively, IO could be produced at concentrations of up to 2 ppt. We consider the reaction of CH_3I with NO_3 to form IO radicals at nighttime over the marine boundary layer. In the present work, the reaction rate constant has been measured using cavity ring-down spectroscopy (CRDS).

$$NO_3 + CH_3I \rightarrow \text{products} \qquad (1)$$

2. Experimental Section

The present CRDS apparatus is similar to that reported previously.[11] Two pulsed lasers were employed. A Nd^{3+}: YAG laser (Continuum, Surelite II) was used to photolyze nitrogen pentoxide (N_2O_5) at 266 nm to generate NO_3 radicals. A dye laser (Sirah Co., Cobra-Stretch; DCM Dye) pumped by the 532 nm output of a Nd^{3+}: YAG laser (Continuum, Surelite I) was used to probe the concentration of NO_3 in the system. After the photolysis laser beam traversed a reaction cell nearly collinear to the axis of the ring-down cavity, the probe laser beam was injected through one of two high-reflectivity mirrors that made up the ring-down cavity. The mirrors (Research Electro Optics) had a specified maximum reflectivity of 0.999 at 635 nm, a diameter of 7.75 mm, a radius of curvature of 1 m, and were mounted 1.04 m apart. Light leaking from one of the mirrors of the ring-down cavity was detected by a photomultiplier tube (Hamamatsu Photonics, R928) through a broad band pass filter (656 nm, fwhm 10 nm). The decay of the light intensity was recorded using a digital oscilloscope (Tektronix, TDS430A) and transferred to a personal computer. The decay of the light intensity is given by the equation

$$I(t) = I_0 \exp(-t/\tau) = I_0 \exp(-t/\tau_0 - \sigma nc(L_R/L)t) \qquad (2)$$

where $I(t)$ is the intensity of light at time t, τ_0 is the cavity ring-down time (10 μs at 662.0 nm) without photolysis laser light, L_R is the length of the reaction region (0.46 m) while L is the cavity length (1.04 m), τ is the cavity ring-down time with photolysis light, n and σ are the concentration and absorption cross section of the species of interest, and c is the speed of light. To measure this absorption spectrum, the broad band pass filter in front of the photomultiplier tube was temporarily removed.

The reaction cell consisted of a Pyrex glass tube (21 mm i.d.), which was evacuated by an oil rotary pump attached with a liquid N_2 trap. The temperature of the gas flow region was controlled by circulation of thermostated water and was kept at 298 K. The difference between the temperatures of the sample gas at the entrance and exit of the flow region was < 0.1 K. The pressure in the cell was monitored by an absolute pressure gauge (MKS, Baratron). Gas flows were measured and regulated by mass flow controllers (KOFLOC, model 3660). A slow flow of nitrogen diluent gas was introduced at both ends of the ring-down cavity close to the mirrors to minimize deterioration caused by exposure to reactants and products. The total flow

* Corresponding author. E-mail: yukio_n@im.hiroshima-cu.ac.jp Fax: +81-82-830-1825.

10.1021/jp051817n CCC: $30.25
Published on Web 06/30/2005

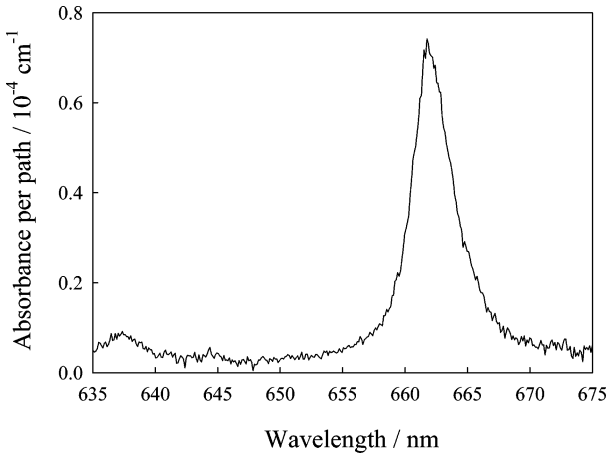

Figure 1. Absorption spectrum of NO_3 measured with our cavity ring-down spectrometer for $[N_2O_5] = 1.3 \times 10^{15}$ molecules cm^{-3} in 100 Torr of N_2 diluent.

rate was kept constant at 1.0×10^3 cm^3 min^{-1} (STP). Experiments were performed with 1−2 Hz laser operation.

NO_3 radicals were produced by the photolysis of N_2O_5 ($(1-3) \times 10^{15}$ molecules cm^{-3}) at 266 nm in 20−200 Torr of N_2 diluent. The absorption cross-section $\sigma_{N_2O_5}$ at 266 nm is 2.0×10^{-19}cm^2 molecule^{-1}.[12]

$$N_2O_5 + h\nu(266\ \text{nm}) \rightarrow NO_3 + NO_2 \qquad (3)$$

The electronic transition $NO_3(B^2E' \leftarrow X^2A'_2)$ was monitored at 662.0 nm. The absorption of NO_3 was converted to the concentration by using the reported absorption cross section at 662 nm, $\sigma_{NO_3} = 2.0 \times 10^{-17}$ cm^2 molecule^{-1}.[12−15] Signal decays of NO_3 in the presence of excess CH_3I provide kinetic data for the reaction of $NO_3 + CH_3I$. Uncertainties reported herein are one standard deviation.

N_2O_5 was synthesized according to a reported method as follows.[16] Concentrated nitric acid (HNO_3) in a glass flask was cooled to dry ice temperature. While ozone in an oxygen stream was passed through the flask, P_2O_5 was added into the flask. Then, N_2O_5 gas evolved and was collected in a cold trap at dry ice temperature. The condensation was fractionated by vacuum distillation to remove N_2O_4 from N_2O_5. Other reagents were obtained from commercial sources. CH_3I (99.0%) was subjected to repeated freeze−pump−thaw cycles before use. N_2 (> 99.9995%) and O_2 (> 99.995%) were used without further purification.

3. Results and Discussion

3.1. Determination of the Rate Constants of $NO_3 + CH_3I$ in 20−200 Torr of N_2 diluent. Figure 1 shows the absorption spectrum of NO_3 from the photolysis of N_2O_5 at 266 nm in 100 Torr of N_2 diluent. Although the photolysis of N_2O_5 generates NO_2, the absorption spectrum shows that there is no observable absorption of NO_2 in this wavelength range. Decay profiles of NO_3 in the absence of CH_3I were monitored at 662 nm for the concentration range of $[NO_3]_0 = (2-5) \times 10^{12}$ molecules cm^{-3}. The measured decay profiles of NO_3 were well reproduced by single-exponential decay curves that are expressed by eq 4 with $k' = (6.5 \pm 0.5) \times 10^2$ s^{-1}.

$$[NO_3]_t = [NO_3]_0 \exp(-k't) \qquad (4)$$

Although possible reaction pathways (reactions 5−7) responsible for the decay of NO_3 are listed below, the contributions of reactions 5 and 6 are found to be very small in the decay process of NO_3 under the present experimental conditions, using the previously reported rate constants for reactions 5, 6a, and 6b at 298 K (Table 1).[12,17,18]

TABLE 1: Rate Constants Used for Calculation of Temporal Change of NO_3 at 298 K

reaction	rate constant/cm^3 molecule^1 s^{-1}	reference
1	$(4.1 \pm 0.2) \times 10^{-13}$	present study
5	2.3×10^{-16}	[12, 17]
6a	6.6×10^{-16}	[12]
6b[a]	8.5×10^{-13}	[18]
9	$(3.5 \pm 1.0) \times 10^{-11}$	[19]
10	$(4.5 \pm 1.9) \times 10^{-10}$	[20]
10[b]	1.6×10^{-11}	[12, 18, 24]
12	$(9.96 \pm 4.98) \times 10^{-12}$	[25]
13	$(3.26 \pm 0.40) \times 10^{-11}$	[26]
14[a]	3.2×10^{-14}	[27]
15[a]	8.6×10^{-11}	[18]
17[a]	5.1×10^{-13}	[12]
18	1.3×10^{-12}	[18]

[a] In 100 Torr of N_2 diluents. [b] The rate constant of $NO_3 + Br$ is adopted for $NO_3 + I$. See the text.

$$NO_3 + NO_3 \rightarrow \text{products} \qquad (5)$$

$$NO_3 + NO_2 \rightarrow NO + NO_2 + O_2 \qquad (6a)$$

$$NO_3 + NO_2 + M \rightarrow N_2O_5 + M \qquad (6b)$$

$$NO_3 \rightarrow \text{diffusion and wall loss} \qquad (7)$$

To determine the rate constant of NO_3 with CH_3I, temporal profiles of $[NO_3]$ were measured in the presence of CH_3I (up to 3.2×10^{15} molecules cm^{-3}). Since $[CH_3I]_0$ is so much in excess of $[NO_3]_0$ and the photodissociation of CH_3I occurs at 266 nm, the following radical reactions should occur:

$$CH_3I + h\nu(266\ \text{nm}) \rightarrow CH_3 + I \qquad (8)$$

$$NO_3 + CH_3 \rightarrow \text{products} \qquad (9)$$

$$NO_3 + I \rightarrow NO_2 + IO \qquad (10)$$

The reported rate constants for reactions 9 and 10 are listed in Table 1.[19,20] In this table we adopted the reported rate constant of $NO_3 + Br$ for $NO_3 + I$. This is because the rate constants of $NO_3 + F/Cl/Br$ are reported to be $7 \times 10^{-11}/2.4 \times 10^{-11}/1.6 \times 10^{-11}$ cm^3 molecule^{-1} s^{-1}.[12,18,21−24] Thus, the reactivity of halogen atoms for NO_3 is expected to be F > Cl > Br > I. However, the reported rate constant with I atom, $(4.5 \pm 1.9) \times 10^{-10}$ cm^3 molecule^{-1} s^{-1}, is much larger than that expected from this tendency.[20] Since no recommended value is available for the rate constant of $NO_3 + I$ in the databases, we assumed that the rate constant for $NO_3 + I$ is the same as that for $NO_3 + Br$.[12,18] The concentrations of CH_3 and I formed by photolysis are estimated from the photoabsorption cross sections at 266 nm.

$$[CH_3]_0 = [I]_0 = [NO_3]_0 \frac{\sigma_{CH_3I}[CH_3I]}{\sigma_{N_2O_5}[N_2O_5]} \qquad (11)$$

where σ_{CH_3I} and $\sigma_{N_2O_5}$ are 1.0×10^{-18} and 2.0×10^{-19} cm^2 molecule^{-1}, respectively.[12] Thus, $[CH_3]_0$ and $[I]_0$ are estimated to be $5-50 \times 10^{12}$ molecules cm^{-3}. $[NO_3]_0$ was $(3-5) \times 10^{12}$ molecules cm^{-3}. As for CH_3 and I, radical reactions 12−15

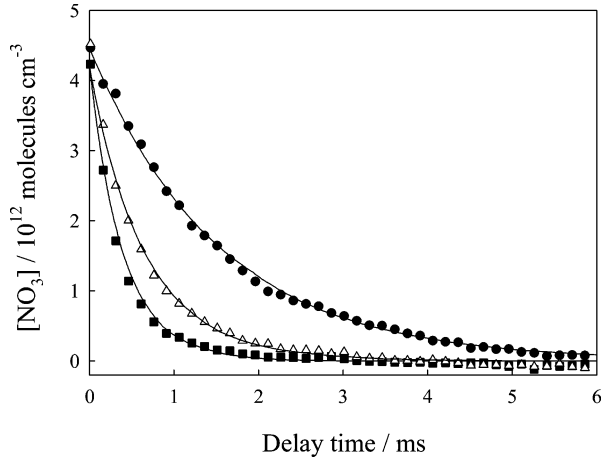

Figure 2. Typical decay profiles of NO_3 with and without CH_3I in 100 Torr of N_2 diluent at 298 K. $[CH_3I]_0 = 0$ (closed circles), 0.81×10^{15} (opened triangles), and 1.6×10^{15} molecules cm^{-3} (closed squares). The solid curve is a fit to the data by a numerical kinetics simulation.

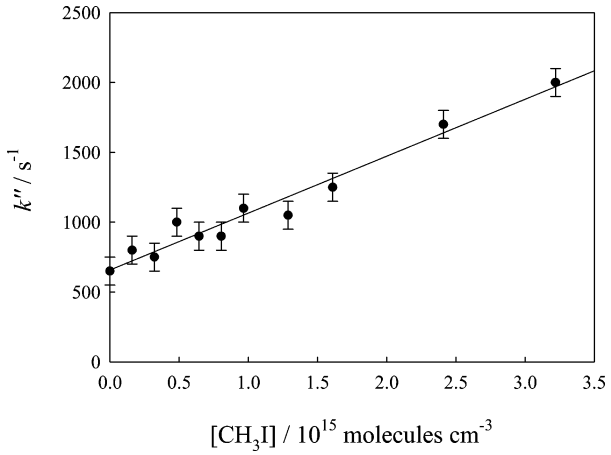

Figure 3. Second-order plots for $NO_3 + CH_3I$ in 100 Torr of N_2 diluent at 298 K. The solid line is the linear least-squares fit.

should occur. The reported rate constants for reactions 12−15 at 298 K are listed in Table 1.[18,25−27]

$$CH_3 + I + M \rightarrow CH_3I + M \quad (12)$$

$$CH_3 + NO_2 \rightarrow \text{products} \quad (13)$$

$$I + I + M \rightarrow I_2 + M \quad (14)$$

$$I + NO_2 + M \rightarrow INO_2 + M \quad (15)$$

To determine the rate constant of $NO_3 + CH_3I$, temporal decay profiles of $[NO_3]$ are simulated with the IBM Chemical Kinetics Simulator Program using reactions 1, 5−7, 9, 10, and 12−15. Typical decays are shown by solid curves in Figure 2 in 100 Torr of N_2 diluent at 298 K; k'' is the pseudo first-order decay parameter of NO_3 for the best fit procedure:

$$k'' = k_1[CH_3I] + k_7 \quad (16)$$

Here, k'' was measured as a function of $[CH_3I]$ and plotted in Figure 3. The linear least-squares analysis gives $k_1 = (4.1 \pm 0.2) \times 10^{-13}$ cm^3 $molecule^{-1}$ s^{-1}. Based on our simulator calculation, the loss of NO_3 via reactions 9 and 10 under the initial conditions ($[CH_3]_0 = [I]_0 = 2.0 \times 10^{13}$ molecules cm^{-3}) was determined to be < 20% and < 9% when NO_3 is completely consumed. Reactions 5, 6, 12, and 14 have a smaller influence on determination of k_1. Similarly, reactions 13 and 15 are minor radical reactions. Thus, reactions 1 and 7 contribute mainly to the decay of NO_3. As will be described below, even when reaction 9 was effectively removed from the reaction mechanism by addition of a radical scavenger gas, O_2, the same rate constant k_1 was obtained. The temporal decay profiles of $[NO_3]$ are also simulated with changing the value of k_{10}. An upper limit value of $k_{10} < 3 \times 10^{-11}$ cm^3 $molecule^{-1}$ s^{-1} was determined.

TABLE 2: Pressure Effect on the Rate Constants of $NO_3 + CH_3I$ at 298 K

pressure of N_2 diluent/Torr	rate constant/cm^3 $molecule^{-1}$ s^{-1}
20	$(4.3 \pm 0.5) \times 10^{-13}$
100	$(4.1 \pm 0.2) \times 10^{-13}$
200	$(4.3 \pm 0.9) \times 10^{-13}$
100 ($N_2/O_2 = 9/1$)	$(4.3 \pm 0.3) \times 10^{-13}$

To test the pressure effect by a diluent gas, additional experiments were performed at 20 and 200 Torr of N_2 diluent. Since reactions 6b, 12, 14, and 15 are termolecular reactions, the rate constants should depend on the total pressure. In our calculation, the rate constants for reactions 6b, 14, and 15 in 20 and 200 Torr of N_2 diluent were taken from references 18 and 27. The rate constant for reaction 12, k_{12}, was assumed to increase linearly with total pressure. Actually, the results were not sensitive to k_{12}. Consequently, we obtain $k_1 = (4.3 \pm 0.5) \times 10^{-13}$ at 20 Torr, and $k_1 = (4.3 \pm 0.9) \times 10^{-13}$ cm^3 $molecule^{-1}$ s^{-1} at 200 Torr. These results are summarized in Table 2. Since k_1 is pressure independent for 20−200 Torr, the present value determined in 200 Torr of N_2 is appropriate for use in atmospheric models. In the present study, measurements of the rate constants of reaction NO_3 with CH_3I at other temperatures were not performed because the temperature dependence of some reactions used in simulation has not been reported.

3.2. Determination of the Rate Constant of $NO_3 + CH_3I$ in the Presence of O_2. As described above, the reaction of $NO_3 + CH_3$ has a larger influence on the loss of NO_3. For example, the loss of NO_3 via reactions 9 and 10 under the initial conditions ($[CH_3]_0 = [I]_0 = 6.0 \times 10^{12}$ molecules cm^{-3}), which were typical conditions in the determination of the rate constant of $NO_3 + CH_3I$, are determined to be < 11% and < 5% in the presence of O_2 by our simulator calculation. Therefore, CH_3 radicals were converted to CH_3O_2 by addition of 10 Torr O_2 to remove the influence of CH_3 on the loss mechanism of NO_3.

$$CH_3 + O_2 + M \rightarrow CH_3O_2 + M \quad (17)$$

The reported rate constant of reaction 17 at 298 K in 100 Torr of N_2 diluent is $k_{17} = 5.1 \times 10^{-13}$ cm^3 $molecule^{-1}$ s^{-1}. Based on the rate constant, O_2 scavenges CH_3 radicals within 7 μs after the photolysis laser pulse.

$$NO_3 + CH_3O_2 \rightarrow NO_2 + CH_3O + O_2 \quad (18)$$

The rate constant of reaction 18 is reported to be $k_{18} = 1.3 \times 10^{-12}$ cm^3 $molecule^{-1}$ s^{-1}.[18] Using these rate constants, the influence of CH_3O_2 on the loss of NO_3 could be neglected. Under these conditions, NO_3 radicals are lost only via reactions 1 and 7. Figure 4 shows the decay profiles of NO_3 with and without CH_3I in 10 Torr of O_2 and 90 Torr of N_2 diluent at 298 K. $[CH_3I]_0$ was 1.6×10^{15} molecules cm^{-3}. The decay curves of NO_3 were analyzed as first-order decay kinetics with use of eq 4 under these conditions. Here, k' is approximated by the sum of the rate constants for the loss of NO_3 via reactions 1 and 7. Typical examples of the temporal profiles are shown in Figure 4 with use of eq 4. The value of k_7 was determined before

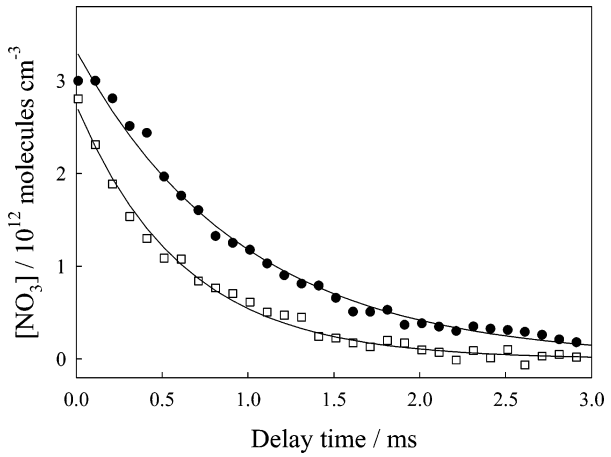

Figure 4. Typical decay profiles of NO_3 with and without CH_3I in 10 Torr of O_2 and 90 Torr of N_2 diluent at 298 K. $[CH_3I]_0 = 1.6 \times 10^{15}$ molecules cm^{-3}. The solid curve is a fit of eq 4 to the data.

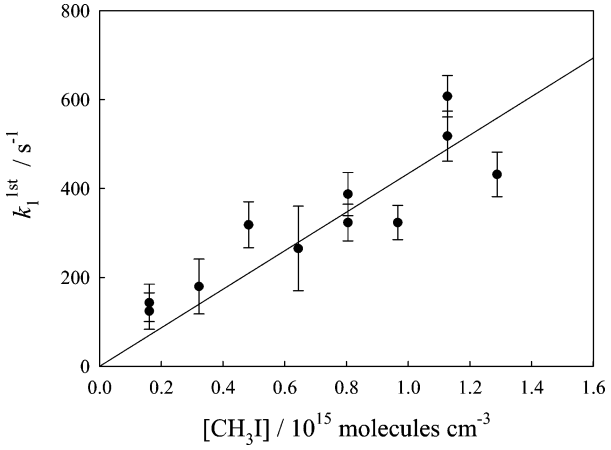

Figure 5. Second-order plots for $NO_3 + CH_3I$ in 10 Torr of O_2 and 90 Torr of N_2 diluent at 298 K. The solid line is the linear least-squares fit.

and after the measurements in the absence of CH_3I. By these procedures, the pseudo-first-order rate losses of NO_3 via reaction 1, k_1^{1st}, could be extracted from the observed k'.

$$k_1^{1st} = k' - k_7 \tag{19}$$

$$k_1^{1st} = k_1[CH_3I] \tag{20}$$

Figure 5 shows k_1^{1st} vs $[CH_3I]$. The linear least-squares analysis shows the rate constant of the reaction of NO_3 radicals with CH_3I to be $k_1 = (4.3 \pm 0.3) \times 10^{-13}$ cm^3 $molecule^{-1}$ s^{-1}. This value is in good agreement with the rate constant determined above for 100 Torr of N_2 diluent.

4. Reaction Products and Atmospheric Implications

The products of the reaction of NO_3 radicals with CH_3I will be discussed below. Only the following reaction pathway is exothermic:

$$NO_3 + CH_3I \rightarrow HNO_3 + CH_2I \qquad \Delta H = -3.7 \pm 10.5 \text{ kJ mol}^{-1} \tag{1}$$

Although hydrogen atom abstraction reactions of NO_3 with HCl, CH_2O, and CH_3CHO are reported to be slow, typically 10^{-15}–10^{-17} cm^3 $molecule^{-1}$ s^{-1}, the rate constants of NO_3 with CH_3I, CH_3SCH_3, and CH_3SH are as high as 10^{-12}–10^{-13} cm^3 $molecule^{-1}$ s^{-1}.[12] These fast reactions have negative temperature dependence, suggesting the formation of a short-lived intermediate complex.[28−32] The pressure independence of the rate constants for CH_3I, CH_3SCH_3, and CH_3SH may be explained by a short lifetime of the intermediate complex.

Once CH_2I is formed in the atmosphere, CH_2I reacts with O_2 to form an IO radical.[33]

$$CH_2I + O_2 \rightarrow IO + HCHO \tag{21}$$

The rate constant of reaction 21 is reported to be $(4.0 \pm 0.4) \times 10^{-13}$ cm^3 $molecule^{-1}$ s^{-1}. By combining this rate constant and the concentration of O_2, the atmospheric lifetime of CH_2I determined by this reaction is 0.5 μs. If CH_2I are produced in the atmosphere, those are considered to be consumed by reaction 21 to generate IO radicals. Thus, oxidation of CH_3I by NO_3 results in the formation of IO in the atmosphere.

CH_3I is the most abundant iodine containing compound in the atmosphere. Atmospheric mixing ratio of CH_3I over the open ocean is between 0.5 and 2 pptv, with higher amounts near coastal areas.[34] NO_3 radical is considered to be one of the most important oxidizers, especially in urban areas, because NO_3 is formed by the reaction of NO_2 with O_3. Solar photolysis and the reaction with NO suppress the concentration of NO_3 during the daytime, resulting in the mixing ratio of NO_3 peaking at nighttime. Even in the marine boundary layer, the concentration of NO_3 rises up to 10 pptv at nighttime.[10] Here, the lifetime of CH_3I, with removal via the reaction with NO_3, is estimated to be 3 h by combining the concentration of NO_3 in the marine boundary layer with the rate constant determined in this work. Considering the fact that the photochemical lifetime of CH_3I is a few days, the reaction of CH_3I with NO_3 would play an important role in the formation of the reactive iodine compounds. Hence, the rather high concentration of IO can be rationalized by considering this reaction.

Acknowledgment. The authors thank Dr. S. Hashimoto of Kyoto University and Dr. S. Aloisio of California State University for his help in construction of the apparatus and for valuable discussion, respectively. This work was partly supported by a Grant-in-Aid from the Ministry of Education, Science, Sports and Culture, Japan (No. 16710006) and by the Sasagawa Scientific Research Grant from The Japan Science Society. T.I. and M.K. are grateful to a grant-in-aid in the priority research field "Radical Chain Reactions" from the Ministry of Education, Science, Sports and Culture, Japan. T.I. is also grateful to a grant from Hiroshima City University for Special Academic Research (General Studies).

References and Notes

(1) Alicke, B.; Hebestreit, K.; Stutz, J.; Platt U. *Natur*e **1999**, *397*, 572.

(2) Allan, B.; McFiggans, J. G.; Plane, J. M. C.; Coe, H. *J. Geophys. Res.* **2000**, *105* (D11), 14, 363.

(3) Davis, D. J.; Crawford, J.; Liu, S.; McKeen, S.; Bandy, A.; Thornton, D.; Rowland, F.; Blake D. *J. Geophys. Res.* **1996**, *101* (D1), 2135.

(4) McFiggans, G.; Plane, J. M. C.; Allan, B. J.; Carpenter, L. J.; Coe, H.; O'Dowd, C. D. *J. Geophys. Res.* **2000**, *105* (D11), 14371.

(5) Solomon, S.; Garcia, R. R.; Ravishankara, A. R. *J. Geophys. Res.* **1994**, *99* (D10), 20, 491.

(6) Nakano, Y.; Enami, S.; Nakamichi, S.; Aloisio, S.; Hashimoto, S.; Kawasaki, M. *J. Phys. Chem. A* **2003**, *107*, 6381.

(7) Roehl, C. M.; Burkholder, J. B.; Moortgat, G. K.; Ravishankara, A. R.; Crutzen, P. J. *J. Geophys. Res.* **1997**, *102*, 12819.

(8) Rattigan, O. V.; Shallcross, D. E.; Cox, R. A. *J. Chem. Soc., Faraday Trans.* **1997**, *93*, 2839.

(9) Brown, A. C.; Canosa-Mas, C. E.; Wayne, R. P. *Atmos. Environ.* **1990**, *24A*, 361.

(10) Saiz-Lopez, A.; Plane, J. M. C. *Geophys. Res. Lett.* **2004**, *31*, L04112

(11) Ninomiya, Y.; Hashimoto, S.; Kawasaki, M.; Wallington, T. J. *Int. J. Chem. Kinet*. **2000**, *32*, 125.

(12) Sander, S. P.; Friedl, R. R.; Ravishankara, A. R.; Golden, D. M.; Kolb, C. E.; Kurylo, M. J.; Huie, R. E.; Orkin, V. L.; Molina, M. J.; Moortgat, G. K.; Finlayson-Pitts, B. J. *Chemical Kinetics and Photochemical Data for Use in Stratospheric Modeling: Evaluation 14*, Jet Propulsion Laboratory, California, 2003.

(13) Ravishankara, A. R.; Mauldin, R. L. *J. Geophys. Res.* **1986**, *91*, 8709.

(14) Sander, S. P. *J. Phys. Chem.* **1986**, *90*, 4135.

(15) Canosa-Mas, C. E.; Fowles, M.; Houghton P. J.; Wayne R. P. *J. Chem. Soc., Faraday Trans. 2* **1987**, *83*, 1465.

(16) Caesar G. V.; Goldfrank M. *J. Am. Chem. Soc*. **1946**, *68*, 372.

(17) Biggs, P.; Canosa-Mas, C. E.; Monks, P. S.; Wayne, R. P.; Benter, Th.; Schindler, R. N. *Int. J. Chem. Kinet.* **1993**, *25*, 805.

(18) Atkinson, R.; Baulch, D. L.; Cox, R. A.; Hampson, R. F., Jr.; Kerr, J. A.; Rossi, M. J.; Troe, J. *IUPAC Summary of Evaluated Kinetic and Photochemical Data for Atmospheric Chemistry*; Appendix; 2000.

(19) Biggs, P.; Canosa-Mas, C. E.; Fracheboud, J.-M.; Shallcross, D. E.; Wayne, R. P. *J. Chem. Soc., Faraday Trans.* **1994**, *90*, 1197.

(20) Chembers, R. M.; Heard, A. C.; Wayne, R. P. *J. Phys. Chem*. **1992**, *96*, 3321.

(21) Rahman, M. M.; Becker, E.; Benter, Th.; Schindler, R. N. *Ber. Bunsen-Ges. Phys. Chem* **1988**, *92*, 91.

(22) Mellouki, A.; Le Bras, G.; Poulet, G. *J. Phys. Chem.* **1987**, *91*, 5760.

(23) Becker, E.; Wille, U.; Rahman, M. M.; Schindler, R. H. *Ber. Bunsen-Ges. Phys. Chem.* **1991**, *95*, 1173.

(24) Mellouki, A.; Poulet, G.; Le Bras, G.; Singer, R.; Burrows, J. P.; Moortgat, G. K. *J. Phys. Chem.* **1989**, *93*, 8017.

(25) Hunter, T. F.; Kristjansson, K. S. *J. Chem. Soc., Faraday Trans II* **1982**, *78*, 2067.

(26) Albaladejo, J.; Jimenez, E.; Notario, A.; Cabanas, B.; Martinez, E. *J. Phys. Chem. A* **2002**, *106*, 2512.

(27) Stephan, K. H.; Comes, F. J. *Chem. Phys. Lett*. **1979**, *65*, 251.

(28) Dlugokencky, E. J.; Howard, C. J. *J. Phys. Chem.* **1988**, *92*, 1188.

(29) Daykin, E. P.; Wine, P. H. *Int. J. Chem. Kinet.* **1990**, *22*, 1083.

(30) Wallington, T. J.; Atkinson, R.; Winer A. M.; Pitts, J. N., Jr. *J. Phys. Chem*. **1986**, *90*, 5393.

(31) Rahman, M. M.; Becker, E.; Benter T.; Schindler, R. N. *Ber. Bunsen-Ges. Phys. Chem.* **1988**, *92*, 91.

(32) MacLeod, H.; Aschmann S. M.; Atkinson, R.; Tuazon, E. C.; Sweetman, J. A.; Winer A. M.; Pitts, J. N, Jr. *J. Geophys. Res.* **1986**, *91*, 5338.

(33) Enami, S.; Ueda, J.; Goto, M.; Nakano, Y.; Aloisio, S.; Hashimoto, S.; Kawasaki, M. *J. Phys. Chem. A* **2004**, *108*, 6347.

(34) Carpenter L. J. *Chem. Rev.* **2003**, *103*, 4953.